Chemistry–A European Journal

Full Paper
doi.org/10.1002/chem.202004619

Chemistry
Europe
European Chemical
Societies Publishing

▌**Biradicals** |*Hot Paper*|

Twisting versus Delocalization in CAAC- and NHC-Stabilized Boron-Based Biradicals: The Roles of Sterics and Electronics

Paul Schmid,[a] Felipe Fantuzzi,[a, b, c] Jonas Klopf,[a] Niklas B. Schröder,[a] Rian D. Dewhurst,[b, c] Holger Braunschweig,[b, c] Volker Engel,[a] and Bernd Engels*[a]

Abstract: Twisted boron-based biradicals featuring unsaturated C_2R_2 (R = Et, Me) bridges and stabilization by cyclic (alkyl)(amino)carbenes (CAACs) were recently prepared. These species show remarkable geometrical and electronic differences with respect to their unbridged counterparts. Herein, a thorough computational investigation on the origin of their distinct electrostructural properties is performed. It is shown that steric effects are mostly responsible for the preference for twisted over planar structures. The ground-state multiplicity of the twisted structure is modulated by the σ framework of the bridge, and different R groups lead to distinct multiplicities. In line with the experimental data, a planar structure driven by delocalization effects is observed as global minimum for R = H. The synthetic elusiveness of C_2R_2-bridged systems featuring N-heterocyclic carbenes (NHCs) was also investigated. These results could contribute to the engineering of novel main group biradicals.

Introduction

Among the various structural motifs adopted by boron centers, the planar, tricoordinate borane (BR_3) is one of the most studied. These compounds are characterized by having an empty p orbital on the boron atom, and several attempts to populate it by chemical reduction or with coordinating Lewis bases and anionic reagents have been made. However, radical anions obtained by addition of a single electron to boranes, which are isoelectronic to neutral, tertiary carbon radicals, are generally highly reactive species, and the synthesis of persistent boron-containing radicals was an arduous challenge for many years.[1] Fortunately, recent advances in the synthesis of boron compounds have paved the way for the generation of distinct

boron radicals stabilized by steric and/or electronic effects, and this has led to a flourishing and active research field.[2]

One of the most successful strategies for the stabilization of main-group radical species is the use of cyclic (alkyl)(amino)carbenes (CAACs) as coordinating ligands. Since their first synthesis and isolation by Bertrand and co-workers in 2005,[3] CAACs have been used for a variety of applications, including: i) the activation of small molecules and chemical bonds;[4] ii) the stabilization of reactive main group and transition metal species;[5] and iii) the development of efficient and robust catalysts for diverse applications.[6] The electronic properties of these singlet carbenes differ significantly from those of conventional (diamino) N-heterocyclic carbenes (NHCs), which are also widely used.[7] The replacement of one of the two π-donating amino substituents of NHCs by the relatively σ-donating but non-π-donating alkyl group of CAACs leads to an increase in both the σ-donor and π-acceptor abilities of the carbene center. Qualitatively, their tendency to stabilize radical species is derived from the so-called captodative effect,[8] wherein the unpaired electron occupies the p orbital of the sp^2-hybridized C^{CAAC} atom and is stabilized by an intricate push–pull mechanism involving the neighboring π-donating N atom (also sp^2-hybridized) and an attached π-acceptor unit (e.g., borane) bound to the carbene. In fact, all-sp^2-hybridized N-C-B moieties have emerged as a promising design principle in computational searches for molecules and materials for use in photochemical and light-harvesting applications.[9]

On going from compounds containing one borane radical to systems with two, the two spin centers can form a closed-shell system if both electrons occupy a stable bonding orbital. Alternatively, they also can exist as biradicals if both electrons occupy two nearly degenerate orbitals. Two noteworthy examples of the latter are CAAC-stabilized bis-borane systems, a

[a] P. Schmid, Dr. F. Fantuzzi, J. Klopf, N. B. Schröder, Prof. V. Engel, Prof. B. Engels
Institute for Physical and Theoretical Chemistry
Julius-Maximilians-Universität Würzburg
Emil-Fischer-Strasse 42, 97074 Würzburg (Germany)
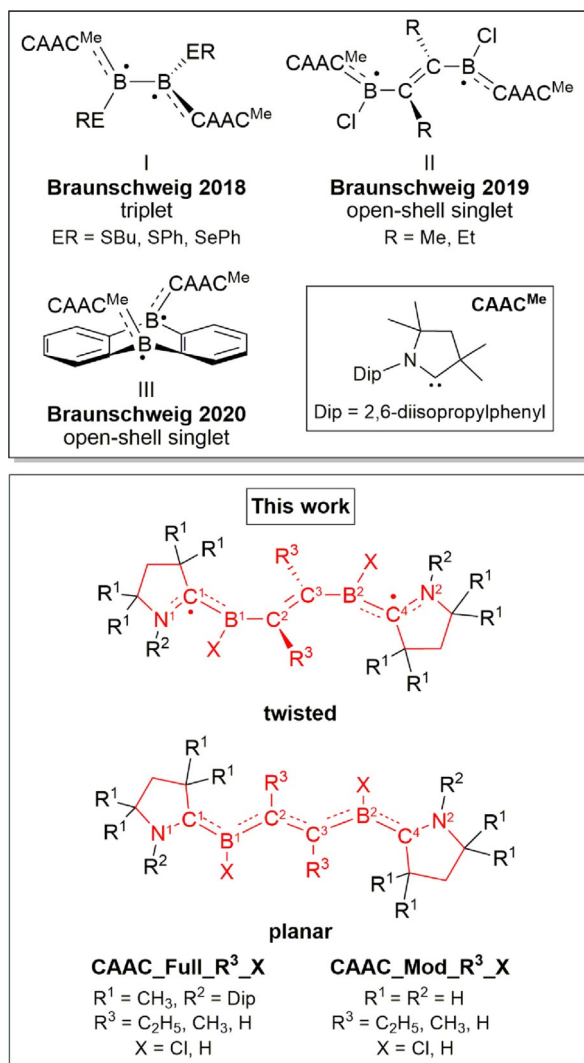E-mail: bernd.engels@uni-wuerzburg.de

[b] Dr. F. Fantuzzi, Dr. R. D. Dewhurst, Prof. H. Braunschweig
Institute for Inorganic Chemistry, Julius-Maximilians-Universität Würzburg
Am Hubland, 97074 Würzburg (Germany)

[c] Dr. F. Fantuzzi, Dr. R. D. Dewhurst, Prof. H. Braunschweig
Institute for Sustainable Chemistry & Catalysis with Boron
Julius-Maximilians-Universität Würzburg, Am Hubland
97074 Würzburg (Germany)

Chemistry–A European Journal

Full Paper
doi.org/10.1002/chem.202004619

Chemistry Europe
European Chemical
Societies Publishing

number of which consist of two directly connected (CAA-C)(RE)B radical units, namely (CAAC)(RE)B–B(ER)(CAAC) (**I**, Scheme 1, ER = SBu, SPh, SePh),[10] while other reported examples contain an unsaturated –C(R)=C(R)– bridge between the boron centers: (CAAC)(Cl)B–(RC=CR)–B(Cl)(CAAC) (**II**; Scheme 1; R = CH$_3$, C$_2$H$_5$).[11] A further example has been published recently, namely a CAAC-stabilized 9,10-diboraanthracene (**III**, Scheme 1).[12] All of these examples have biradical ground states (either singlet or triplet) and adopt different geometries than their closed-shell counterparts. In the directly

connected (CAAC)(RE)B–B(ER)(CAAC) biradicals, for example, the planar (CAAC)(ER)B units are mutually orthogonal, precluding the presence of a B–B π bond.[10] This molecule has a triplet ground state. In the bridged biradicals (CAAC)(Cl)B–(RC=CR)–B(Cl)(CAAC), the RC=CR units are effectively orthogonal to the planar B(Cl)(CAAC) units.[11] Finally, CAAC-stabilized 9,10-diboraanthracene adopts a butterfly shape, which takes the BCN π system out of the plane of the adjacent phenylene groups.[12] Both last-named systems have singlet ground states, but the triplet states are so close in energy that signals can be observed in their EPR spectra. In contrast to the CAAC systems, the corresponding NHC-stabilized 9,10-diboraanthracene and (NHC)(ER)B–B(ER)(NHC) compounds adopt structures that allow the formation of stabilized HOMOs. The former adopts a nearly flat structure,[13] while in the latter the (RE)B–B(ER) unit is planar with distinct B=B bond. The NHC moieties are twisted with respect to this plane by 90°.

While experimental work unambiguously determined the differences in structures and electronic characters between the CAAC- and NHC-stabilized congeners, the reasons for the differences were unclear. This was remedied in the case of the L(RE)B–B(ER)L systems by computational comparison of the two sets of compounds, which showed that the stronger steric demands of the NHCs are important, but the lower-lying triplet states of the CAAC congeners are an essential prerequisite for the formation of biradical ground states.[14]

The present study extends these investigations to the bisborane systems (L)(X)B–(RC=CR)–B(X)(L) in which the borane moieties are bridged by an unsaturated C$_2$R$_2$ group. Remarkably, for L = CAAC, X = Cl, and R = CH$_3$, C$_2$H$_5$, the central olefinic bridge is maintained perpendicular to the B–CAAC moieties, precluding the presence of π delocalization along the CBCCBC backbone and leading to biradical systems. In addition to investigations of the experimentally isolated systems,[10,11] we used theory to investigate derivatives that are not synthetically accessible. Thereby, we performed a comprehensive exploration of the singlet and triplet states of C$_2$R$_2$-bridged bis-borane compounds, aiming to disentangle steric and electronic effects that drive the preference for molecular twisting over π delocalization in experimentally realized structures, and to find reasons why the nonbridged species (CAAC)(RE)B–B(ER)(CAAC) have triplet ground states, whereas the bridged species (CAAC)(Cl)B–(RC=CR)–B(Cl)(CAAC) have open-shell singlet ground states. To obtain further insights we replaced the boron-bound halo substituents, the alkyl groups of the bridging unit, and the bulky groups attached to the CAAC donors with hydrogen atoms. This diminishes steric effects, so that the electronic contributions come to the fore. Another elegant method to disentangle steric and electronic effects was described by Bickelhaupt et al. in 2006.[15] Additionally, we characterized the experimentally unknown NHC counterparts to investigate the generality of the reasons for the differences found for (L)(RE)B–B(ER)(L) and why their syntheses may have failed.

Scheme 1. Top: experimentally realized compounds **I**,[10] **II**,[11] and **III**.[12] Bottom: structures studied herein. The combinations of substituents R^1 and R^2 are denoted *Full* (R^1 = CH$_3$, R^2 = Dip) or *Model* (Mod; R^1 = R^2 = H), while the substituents R^3 and X are explicitly given. For example, the compound with R^1 = CH$_3$, R^2 = Dip, R^3 = CH$_3$, and X = Cl is abbreviated as **CAAC_Full_CH$_3$_Cl**, while that with R^1 = H, R^2 = H, R^3 = H, and X = H is labeled **CAAC_Mod_H_H**. In the planar geometry the dihedral angles φ(N^{1}C^{1}B^{1}C^2), φ(C^{1}B^{1}C^{2}C^3), φ(B^{1}C^{2}C^{3}B^2), φ(C^{2}C^{3}B^{2}C^4), and φ(C^{3}B^{2}C^{4}N^2) are equal to 180°. For the twisted geometry, the dihedral angles φ(N^{1}C^{1}B^{1}C^2), φ(B^{1}C^{2}C^{3}B^2), and φ(C^{3}B^{2}C^{4}N^2) are equal to 180°, while φ(C^{1}B^{1}C^{2}C^3) = −90° and φ(C^{2}C^{3}B^{2}C^4) = 90°. Further geometrical data are summarized in Tables S1–S5 of the Supporting Information. The corresponding dihedral angles for the fully optimized structures are given in Table S4 of the Supporting Information. See text for more details.

Chemistry–A European Journal

Full Paper
doi.org/10.1002/chem.202004619

Chemistry Europe
European Chemical
Societies Publishing

Computational Details

The geometries of the *Full* and *Model* systems were optimized by using the MN12L functional[16] in the spin-unrestricted formalism in conjugation with the 6-311G(d,p) basis set.[17] The computations were performed in vacuum, since the experiments were done in nonpolar solvents.[11] In the following discussion, geometries obtained from optimizations without restrictions are described as "fully optimized" (full-opt). For the singlet states the broken-symmetry method was employed. The relative energies are based on the values of the UMN12L/6-311G(d,p) calculations as well. Such single-reference approaches are often sufficiently accurate.[18] However, for biradicals with small singlet–triplet (S–T) gaps, multireference approaches are needed to obtain accurate potential-energy surfaces (PESs),[19] electronically excited states,[20] or even properties.[21] Hence, the energies of the model systems were also calculated with NEVPT2[22]/cc-pVDZ,[23] which is based on a CASSCF(4,6) calculation.[24]

Tables 1 and 2 give computed $\langle S^2 \rangle$ expectation values of the total spin (see Supporting Information Equation S1)[25] as they provide valuable information about the character of the states and the quality of the computations. Spin-restricted approaches such as CASSCF or NEVPT2 give the correct $\langle S^2 \rangle$ values of 0 for singlet states $[\langle S^2 \rangle = S(S+1)]$, irrespective of whether a closed-shell or an open-shell state is described. In turn, $\langle S^2 \rangle = 2$ is obtained for triplet states. Since such approaches are too computationally expensive, we employed less-expensive spin-unrestricted (also called broken-symmetry) one-determinant DFT approaches for the full systems. These give $\langle S^2 \rangle = 0$ for singlet closed-shell systems, but $\langle S^2 \rangle = 1$ for singlet open-shell systems, because in such one-determinant approaches an open-shell biradical wave function represents a complete mixture of the correct singlet and triplet wave functions. For perfect biradicals the accompanying error in the energy is small because the S–T gap is small. The error can increase for open-shell systems with larger S–T gaps. In spin-unrestricted approaches

errors often also arise from spin contamination, for which the wave function contains artificial contributions from higher spin multiplicities. Hence, the computed $\langle S^2 \rangle$ values not only give information about the character of the state (closed versus open-shell singlet versus triplet), but also offer insights into the quality of the computations, because deviations from the expected $\langle S^2 \rangle$ values indicate problems in the calculations. The singlet open-shell character y was also estimated by the Yamaguchi formula, whereby a closed-shell singlet state is represented by $y = 0$ and an open-shell biradical singlet or triplet by $y = 1$ (see Equation S1 in the Supporting Information).[26] For the C_2R_2-bridged systems the adiabatic S–T gaps were calculated. For the saturated hydrocarbon-bridged systems the calculated S–T gaps are the vertical ones (i.e., obtained by changing the spin state with a fixed geometry), and the NEVPT2/cc-pVDZ calculations were based on a CASCI with an active space size of (2,2). The DFT calculations were carried out with Gaussian 16[27] and the NEVPT2 calculations were performed with ORCA 4.1.1.[28]

Results and Discussion

The experimentally realized molecules **CAAC_Full_CH3_Cl** and **CAAC_Full_C2H5_Cl** adopt twisted geometrical structures in the solid state, leading to open-shell biradical ground states. In both cases a singlet ground state is found, while the corresponding triplet state lies slightly higher in energy. Various effects disfavor the planar arrangement, despite the fact that it would allow extended π delocalization over the C_2R_2 bridge. The twisting may result from the core of the molecule being quite sterically crowded. The underlying steric effects comprise interactions between the methyl groups of the C_2R_2 bridge and the chloro substituent or effects resulting from the CAAC substituents. Additionally, electronic effects similar to those found in the related CAAC- and NHC-stabilized diborenes might contribute.[14] To obtain initial insights into these various effects, we replaced the alkyl substituents of the C_2R_2 bridge, the boron-bound chloro substituents, and the peripheral CAAC substituents consecutively by hydrogen atoms and compared the computed energy differences between the planar and twisted structures ($\Delta E_{p \to t}$). In the planar geometry the dihedral angles $\varphi(N^1C^1B^1C^2)$, $\varphi(C^1B^1C^2C^3)$, $\varphi(B^1C^2C^3B^2)$, $\varphi(C^2C^3B^2C^4)$, and $\varphi(C^3B^2C^4N^2)$ are constrained to 180° while all other geometrical parameters are optimized. Note that these restrictions enforce a planar orientation of the backbone consisting of N^1, C^1, B^1, C^2, C^3, B^2, C^4, and N^2, but do not force the substituents of the C_2R_2 bridge ($R^3 = C_2H_5$, CH_3, H) into the same plane. For the twisted geometry, the dihedral angles $\varphi(N^1C^1B^1C^2)$, $\varphi B^1C^2C^3B^2)$, and $\varphi(C^3B^2C^4N^2)$ are constrained to 180°, while $\varphi(C^1B^1C^2C^3) = -90°$ and $\varphi(C^2C^3B^2C^4) = 90°$. Again, all other geometrical parameters are optimized. The global minimum of a given compound was obtained by geometry optimization without constraints (full-opt). The corresponding dihedral angles for these fully optimized structures are given in Table S4 of the Supporting Information. Variations in the geometrical parameters are listed in Tables S1–S3 of the Supporting Information. The energy data are summarized in Tables 1 and 2. In all cases we give the relative energy with respect to the singlet state of the planar structure to introduce a clear sign convention. For the

Table 1. UMN12L/6-311G(d,p) relative electronic energies [kcal mol⁻¹] of the singlet (S_0) and triplet (T_0) states of the **CAAC_Full_R³_X** systems, where zero is defined as the S_0 state of the planar structures.[a]

System	S_0	T_0	S–T gap	$\langle S^2 \rangle$ (S_0)
CAAC_Full_C2H5_Cl (full-opt)	−42.4	−42.3	0.1	1.01
CAAC_Full_C2H5_Cl (twisted)	−41.5	−41.4	0.1	1.00
CAAC_Full_C2H5_Cl (planar)	0.0	1.2	1.2	0.93
CAAC_Full_CH3_Cl (full-opt)	−34.1	−33.5	0.6	0.97
CAAC_Full_CH3_Cl (twisted)	−32.4	−31.8	0.6	0.98
CAAC_Full_CH3_Cl (planar)	0.0	2.3	2.3	0.77
CAAC_Full_H_Cl (full-opt)	−2.1	9.0	11.1	0.00
CAAC_Full_H_Cl (twisted)	17.7	17.7	0.0	1.01
CAAC_Full_H_Cl (planar)	0.0	11.2	11.2	0.00
CAAC_Full_C2H5_H (full-opt)	−8.3	−7.9	0.4	0.99
CAAC_Full_C2H5_H (twisted)	−7.6	−7.4	0.2	1.01
CAAC_Full_C2H5_H (planar)	0.0	12.8	12.8	0.02
CAAC_Full_CH3_H (full-opt)	−5.1	−4.5	0.6	0.98
CAAC_Full_CH3_H (twisted)	−4.5	−3.8	0.7	0.98
CAAC_Full_CH3_H (planar)	0.0	11.4	11.4	0.00
CAAC_Full_H_H (full-opt)	−1.0	11.0	12.0	0.00
CAAC_Full_H_H (twisted)	23.3	23.4	0.1	1.01
CAAC_Full_H_H (planar)	0.0	12.1	12.1	0.00

[a] Planar-to-twisted energies $\Delta E_{p \to t}$ can be obtained by comparing the energies of the respective planar and twisted structures. A positive value of $\Delta E_{p \to t}$ indicates that the planar structure is more stable. S–T gaps and the $\langle S^2 \rangle$ values (for S_0) are also shown.

Chemistry–A European Journal

Full Paper
doi.org/10.1002/chem.202004619

Chemistry
Europe
European Chemical
Societies Publishing

Table 2. Relative electronic energies [kcal mol^{-1}] of the singlet (S$_0$) and triplet (T$_0$) states of the **CAAC_Mod_R³_X** systems, where zero is defined as the S$_0$ state of the planar structures.[a] $\Delta E_{p \to t}$, S–T gaps, y (for S$_0$), and the $\langle S^2 \rangle$ values (for S$_0$) are also shown.

System	NEVPT2(4,6)/cc-pVDZ				UMN12L/6-311G(d,p)			
	S$_0$	T$_0$	S–T gap	y (S$_0$)	S$_0$	T$_0$	S–T gap	$\langle S^2 \rangle$ (S$_0$)
CAAC_Mod_C$_2$H$_5$_Cl (twisted)	−3.7	−3.3	0.4	0.86	−0.9	−0.6	0.3	0.98
CAAC_Mod_C$_2$H$_5$_Cl (planar)	0.0	10.9	10.9	0.08	0.0	10.5	10.5	0.00
CAAC_Mod_CH$_3$_Cl (twisted)	3.5	3.9	0.4	0.84	3.5	4.0	0.5	0.97
CAAC_Mod_CH$_3$_Cl (planar)	0.0	10.6	10.6	0.09	0.0	10.5	10.5	0.00
CAAC_Mod_H_Cl (twisted)	22.6	22.5	−0.1	0.96	29.0	29.0	0.0	1.01
CAAC_Mod_H_Cl (planar)	0.0	11.2	11.2	0.07	0.0	13.6	13.6	0.00
CAAC_Mod_C$_2$H$_5$_H (twisted)	14.2	14.7	0.5	0.84	15.1	15.6	0.5	0.98
CAAC_Mod_C$_2$H$_5$_H (planar)	0.0	15.7	15.7	0.11	0.0	12.2	12.2	0.00
CAAC_Mod_CH$_3$_H (twisted)	13.1	13.5	0.4	0.81	15.9	16.6	0.7	0.97
CAAC_Mod_CH$_3$_H (planar)	0.0	14.7	14.7	0.08	0.0	11.9	11.9	0.00
CAAC_Mod_H_H (twisted)	27.2	26.9	−0.3	0.96	27.2	27.2	0.0	1.01
CAAC_Mod_H_H (planar)	0.0	11.9	11.9	0.07	0.0	13.9	13.9	0.00

computations we used NEVPT2/cc-pVDZ and UMN12L/6-311G(d,p). The former is a multireference approach and is hence able to describe open-shell biradical structures very accurately. However, it is too demanding for the full systems, for which we had to employ DFT methods. We adopted the UMN12L functional herein to directly compare the present results with our previous works.[10,11,14] The computations for the model systems (Table 2), for example, **CAAC_Mod_C$_2$H$_5$_Cl** or **CAAC_Mod_CH$_3$_Cl**, allow reliable comparison of the NEVPT2 and UMN12L results. We assume that calculations using NEVPT2 are more accurate, because UMN12L describes the open-shell S$_0$ state of the biradical twisted structure as a complete mixture of the singlet and triplet states, as indicated by the $\langle S^2 \rangle$ expectation value of 1.0. Furthermore, DFT tends to overestimate the contribution of π delocalization to the stability of a molecule, that is, it should prefer planar structures to some extent.[29] For **CAAC_Mod_C$_2$H$_5$_Cl**, NEVPT2 predicts that the planar structure is about 4 kcal mol^{-1} higher in energy than the twisted one. UMN12L also computes the planar structure to be less stable than the twisted arrangement, but the difference is only about 1 kcal mol^{-1}. For all other model systems, both approaches predict planar structures. However, as anticipated, UMN12L slightly overestimates the energy differences with respect to the twisted structure, that is, slightly favors the planar arrangement. The error bars of UMN12L for the S–T gaps are smaller than those obtained for $\Delta E_{p \to t}$. For the twisted structure of **CAAC_Mod_CH$_3$_Cl**, NEVPT2 predicts an S–T gap of 0.4 kcal mol^{-1}, while UMN12L computes a value of 0.5 kcal mol^{-1}. This energy variation between NEVPT2 and UMN12L is very similar for the other model systems in their twisted structures. For the planar structures, deviations in the S–T gaps between the two methods are about 1–3 kcal mol^{-1}, but in these cases the S–T gaps are around 10–15 kcal mol^{-1}, and are thus considerably larger than those of the twisted structures. Taken together, these results indicate that UMN12L is qualitatively correct for all model systems studied herein. Hence, also for the full systems, UMN12L is expected to give qualitatively correct results, because the size of the effects determining the energy order of the electronic states and geometrical structures are larger than those of the model systems. Benchmark

calculations with RI-NEVPT2(4,6)/def2-SVP additionally showed that the geometries predicted by UMN12L are sufficiently accurate. This is in line with earlier benchmark calculations.[30]

In agreement with the experimental results, UMN12L predicts that **CAAC_Full_C$_2$H$_5$_Cl** and **CAAC_Full_CH$_3$_Cl** have twisted structures and open-shell singlet ground states (S$_0$). The dihedral angles of the fully optimized structure deviate by up to 6° from those of the solid-state structure (Table S4 of the Supporting Information). Such deviations are observed because the system seems to be quite flexible despite the large, bulky substituents. This can be seen in the energy differences between the computed twisted and the fully optimized structures for both systems. Their calculated energies deviate by only 1–2 kcal mol^{-1} despite variations of more than 10° in their dihedral angles (see Table S4 in the Supporting Information). The deviations between measured and computed bond lengths and angles are even smaller (Tables S1–S3 of the Supporting Information). The triplet T$_0$ state of the fully optimized structure of **CAAC_Full_C$_2$H$_5$_Cl** (**CAAC_Full_CH$_3$_Cl**) lies about 0.1 kcal mol^{-1} (0.6 kcal mol^{-1}) higher in energy than the singlet state. Their multiplicities stand in contrast to the recently investigated CAAC-stabilized diborenes.[10,14] These compounds are also twisted and show an open-shell electronic structure, but have triplet ground states.

The planar structure of **CAAC_Full_CH$_3$_Cl** is about 34 kcal mol^{-1} higher in energy than the fully optimized one. The latter resembles the twisted structure, which is less than 2 kcal mol^{-1} higher in energy. For **CAAC_Full_C$_2$H$_5$_Cl** the corresponding planar structure is even higher in energy, lying 42 kcal mol^{-1} above the fully optimized one. To investigate the underlying reasons for these energy differences the C$_2$H$_5$, CH$_3$, and Cl substituents and the CAAC units were consecutively replaced by hydrogen atoms (Tables 1 and 2). If we replace the CH$_3$ groups of the C$_2$R$_2$ bridge with hydrogen atoms (**CAAC_Full_CH$_3$_Cl** → **CAAC_Full_H_Cl**), the computations predict that the planar structure becomes about 18 kcal mol^{-1} lower in energy than the twisted one. The fully optimized structure closely resembles the planar structure, which is only about 2 kcal mol^{-1} higher in energy. This is in line with experimental X-ray data of the corresponding molecule.[31] As expected, the planar and

Chemistry–A European Journal

Full Paper
doi.org/10.1002/chem.202004619

Chemistry
Europe
European Chemical
Societies Publishing

the fully optimized structure of **CAAC_Full_H_Cl** has a closed-shell S_0 ground state with an S–T gap of about 11 kcal mol^{-1} (UMN12L).

Considering that the planar structure is stabilized by delocalization over the C_2R_2 bridge, steric interactions are essentially responsible for the adoption of twisted structures in the derivatives with alkyl substituents at the C_2R_2 bridge ($R^3 = CH_3$, C_2H_5). The steric demands result from interaction between the R^3 substituents on one side with the boron-bound chlorine atoms, and with the methyl substituents of CAAC moieties ($R^1 = CH_3$) on the other side. Additionally, interactions between $R^2 = Dip$ and R^3 may also contribute. Interactions between $R^2 = Dip$ and $X = Cl$ or H are also expected, but they do not change on going from the twisted to the planar structure. Hence, the preference for twisted or planar structures directly results from the interplay of the stabilization resulting from the delocalization over the planar structure and the strain effects, which decrease significantly on going from the planar to the twisted structure. This higher strain in the planar system arises from all substituents effectively lying in one plane. In contrast, for the twisted structure the distances increase because the R^3 alkyl substituents stay perpendicular with respect to the other bulky groups. To quantify the various effects we used the UMN12L/6-311G(d,p) approach, because NEVPT2 turned out to be too computationally expensive for the full systems.

The magnitude of the stabilization effects resulting from delocalization are best estimated by comparing the energy difference between the twisted and planar structures ($\Delta E_{p\rightarrow t}$) for **CAAC_Mod_H_H**, because in this truncated model, steric effects are diminished as far as possible. The difference is about 27 kcal mol^{-1} in favor of the planar structure. For **CAAC_Mod_CH$_3$_H** and **CAAC_Mod_C$_2$H$_5$_H**, $\Delta E_{p\rightarrow t}$ decreases to about 15–16 kcal mol^{-1}, that is, the steric interactions between $X = H$ and the R^3 alkyl substituents of the C_2R_2 bridge alone amount to approximately 11–12 kcal mol^{-1}. Since $R^1 = R^2 = H$ for Mod systems, their steric demands should be negligible. On going from $X = H$ to $X = Cl$, $\Delta E_{p\rightarrow t}$ changes to approximately $+29$, $+4$, and -1 kcal mol^{-1} for $R^3 = H$, CH_3, and C_2H_5, respectively. This shows that alkyl groups at the C_2R_2 bridge are essential to make the twisted structure competitive. This same conclusion is reached when analyzing **CAAC_Full_H_Cl**, which, in contrast to the alkyl-substituted systems **CAAC_Full_CH$_3$_Cl** and **CAAC_Full_C$_2$H$_5$_Cl**, adopts the planar structure.

For **CAAC_Full_CH$_3$_Cl** and **CAAC_Full_C$_2$H$_5$_Cl** the steric interactions are so strong that restraining $\varphi(N^1C^1B^1C^2)$, $\varphi(C^1B^1C^2C^3)$, $\varphi(B^1C^2C^3B^2)$, $\varphi(C^2C^3B^2C^4)$, and $\varphi(C^3B^2C^4N^2)$ to 180° is not sufficient to enforce a completely planar structure, although it forces the backbone consisting of N^1, C^1, B^1, C^2, C^3, B^2, C^4, and N^2 (see Scheme 1) into a planar orientation. However, the systems use the remaining freedom to move the R^3 alkyl substituents below or above this plane. For **CAAC_Full_C$_2$H$_5$_Cl** a value of $\varphi(C^1B^1C^2C^{R3})$ of about 43° is predicted. The resulting pyramidalization of the C^2 and C^3 centers reduces the strain because the distances between the R^3 and R^1 substituents increase, as is obvious from Figure S1 of the Supporting Information, which shows the computed planar structure for **CAAC_Full_CH$_3$_Cl**. The corresponding distances are given in

Table S5 of the Supporting Information. The pyramidalization should additionally destabilize the system because two sp^3 carbon centers are formed, breaking the C–C double bond and allowing biradical character to emerge. The formation of two sp^3 centers is proven by the sums of the bond angles around C^2 and C^3 (Table S3 of the Supporting Information). For the fully optimized structure of **CAAC_Full_C$_2$H$_5$_Cl** the sum of the angles around the C^2 center is 359.8°, which nicely agrees with the 360° expected for a planar sp^2-hybridized carbon center. In contrast, for the planar structure the sum is only 346.6°. For **CAAC_Full_CH$_3$_Cl** similar values are found. For the planar conformer of **CAAC_Full_H_Cl** the sum is again 359.8°. The biradical character of the corresponding systems (Table 1, see **CAAC_Full_CH$_3$_Cl** (planar) and **CAAC Full C$_2$H$_5$ Cl** (planar) entries) becomes obvious from the computed $\langle S^2 \rangle$ values (0.77 and 0.93) and the small S–T gaps (2.3 and 1.2 kcal mol^{-1}). For completely planar structures [e.g., **CAAC_Mod_H_H** (planar), see Table 2] the $\langle S^2 \rangle$ values are 0, and considerably larger S–T gaps (e.g., 14 kcal mol^{-1}) are computed. By combining $\Delta E_{p\rightarrow t}$ for **CAAC_Full_C$_2$H$_5$_Cl** (-42 kcal mol^{-1}) and **CAAC_Full_CH$_3$_Cl** (-32 kcal mol^{-1}) with the values estimated for the stabilization effects resulting from the delocalization (≈ 27 kcal mol^{-1}), the steric effects in **CAAC_Full_C$_2$H$_5$_Cl** (planar) and **CAAC_Full_CH$_3$_Cl** (planar) can be estimated to be at least 70 and 60 kcal mol^{-1}, respectively. These values only represent lower bounds, because they neglect effects resulting from the formation of biradical species in **CAAC_Full_CH$_3$_Cl** (planar) and **CAAC_Full_C$_2$H$_5$_Cl** (planar).

To summarize, the strain effects leading to the twisted structures of **CAAC_Full_CH$_3$_Cl** and **CAAC_Full_C$_2$H$_5$_Cl** are greater than 60 and 70 kcal mol^{-1}, respectively. Alkyl substituents at the C_2R_2 bridge are mainly responsible for the twisting, as **CAAC_Full_H_Cl** adopts a planar structure, which is computed to be approximately 18 kcal mol^{-1} more stable than the twisted structure. By comparing this value with the stabilization estimated by delocalization (≈ 27 kcal mol^{-1}), it becomes obvious that, even for **CAAC_Full_H_Cl**, steric effects should play a role. Indeed, the distances between the $X = Cl$ atom and the C_2H_2 hydrogen atoms, and between the $R^1 = CH_3$ groups of the CAAC and the C_2H_2 hydrogen atoms, are still about 0.2 Å smaller than the van der Waals radii (Table S5, Figure S1 of the Supporting Information). Nevertheless, the resulting repulsions are overcompensated by the stabilization resulting from the delocalization. For completely planar systems with $R^3 = $ alkyl, the corresponding distances would be considerably shorter than their respective van der Waals radii, so that the resulting strain cannot be overcompensated.

In contrast to the biradical congeners of CAAC-stabilized diborenes, which have open-shell triplet ground states,[10,14] **CAAC_Full_C$_2$H$_5$_Cl** and **CAAC_Full_CH$_3$_Cl** have open-shell singlet ground states.[12] The similarities and differences of the systems are summarized in Scheme 1. The small S–T gaps of less than 1 kcal mol^{-1} show that in both systems the interactions between the two radical centers are very weak. For the C_2R_2-bridged boron biradicals (Scheme 1, **II**) the π systems of both radical centers have the same alignment, that is, their π systems could interact in principle. However, the interaction is

Chemistry–A European Journal

Full Paper
doi.org/10.1002/chem.202004619

Chemistry
Europe
European Chemical
Societies Publishing

diminished because both radical centers are separated by the twisted C_2R_2 group. For the biradical congeners of the diborenes (Scheme 1, **I**) the interaction between the radical centers is weak because both radical centers are twisted by 90°, so that the π systems of both radical centers are perpendicular to each other. To obtain insight into these interactions, we turn to the data computed for the twisted systems. The twisted orientation is not always the equilibrium geometry; for example, for **CAAC_Mod_H_Cl** the planar structure is more stable. However, by using the computed twisted structures we can extend the investigation of the S–T gaps to include different substituents at the C_2R_2 bridge. Relying on experimental data,[10,11] we could only compare **CAAC_Full_CH₃_Cl** and the biradical congeners of the diborenes for which temperature-dependent measurements were performed.[10,11] Since the S–T gaps are quite small, we used the model systems for this analysis, as they can be characterized by high-level multireference approaches. The computed energies are given in Table 2. The multireference calculations predict singlet ground states for the twisted structures of **CAAC_Mod_C₂H₅_Cl**, **CAAC_Mod_C₂H₅_H**, **CAAC_Mod_CH₃_Cl**, and **CAAC_Mod_CH₃_H**. On replacing the alkyl groups of the bridge with hydrogen atoms, the triplet states become the ground states of such twisted structures. The shapes and the energies of the relevant SOMOs are summarized in Figure 1, which also gives the computed S–T gaps.

According to Hund's rule, molecules in which two electrons occupy two energetically degenerate orbitals should have a triplet ground state. If the energy difference between the orbitals is small but nonzero, the situation becomes more complicated, as excellently described in the reviews of Bonačić-Koutecký, Koutecký, and Michl.[32] These authors coined the expression "biradicaloids" to describe systems with two nearly degenerate orbitals whose energy splitting arises from possible interactions between both radical centers. In biradicaloids three different singlet states and one triplet state have to be considered. Here, we will only briefly reiterate the underlying aspects. More information can be taken from the Supporting Information or from the original reviews.[30]

For orbitals that are delocalized over both spin centers, such as those we obtained for the twisted C_2R_2-bridged diborenes and the biradical congeners of diborene systems (Figure 1), the wave function of the lowest-lying singlet state is dominated by the negative linear combination of the two determinants in which either SOMO1 or SOMO2 is doubly occupied (Scheme S2 of the Supporting Information). This state may be shifted below the triplet state, either due to its interaction with the other two singlet states, or because SOMO1 becomes considerably more stable than SOMO2. With increasing energy difference between the orbitals, the determinant in which SOMO1 is doubly occupied increasingly dominates the wave function of the lower singlet state. Finally, the singlet state moves below
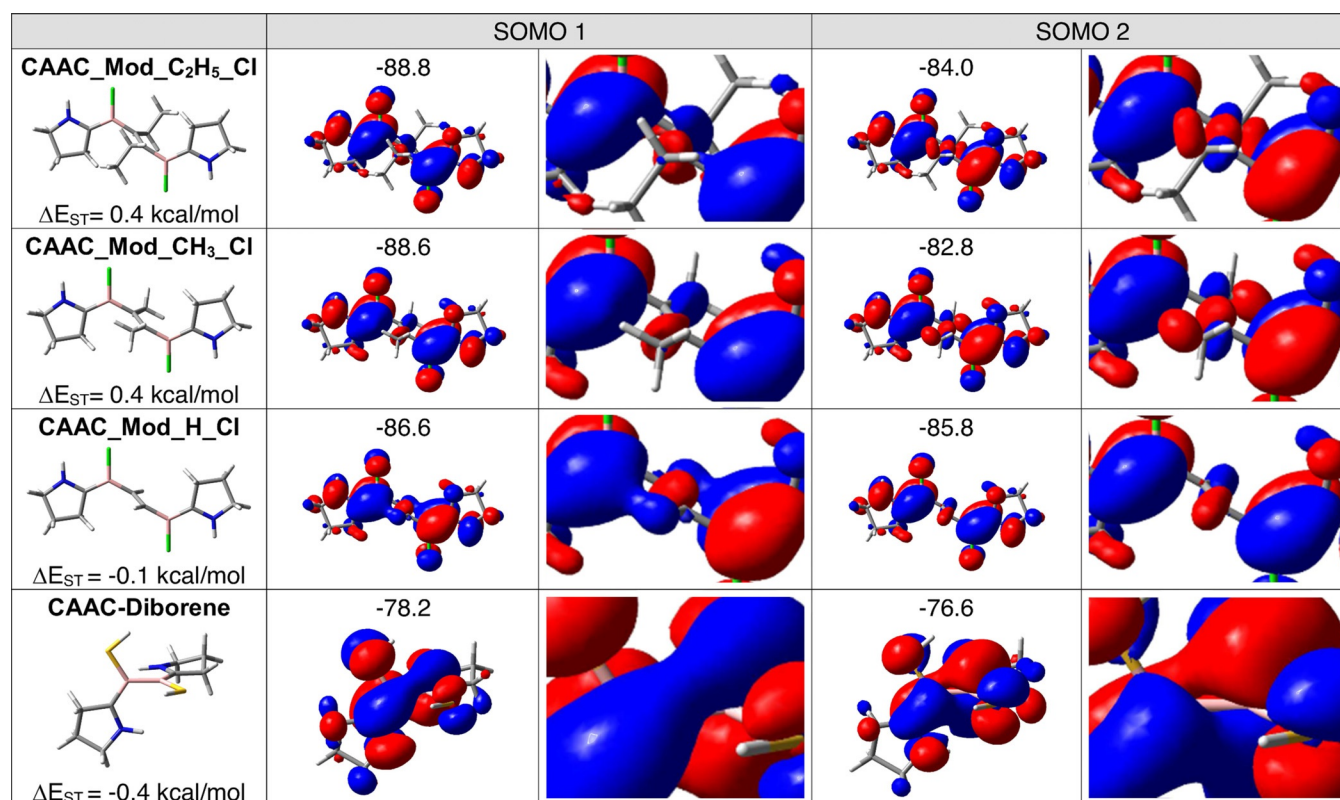
Figure 1. SOMOs of the twisted structures of distinct model C_2R_2-bridged systems and those of the model diborene biradical congener. The triplet orbital energies are given in kcal mol⁻¹. The corresponding CASSCF orbitals possess virtually identical shapes and show the same energy trends (Figures S3, S4 of the Supporting Information). S–T gaps ΔE_{ST} obtained from NEVPT2/cc-pVDZ computations are also given. A positive value means a singlet ground state.

Chemistry–A European Journal

Full Paper
doi.org/10.1002/chem.202004619

Chemistry
Europe
European Chemical
Societies Publishing

the triplet state, in which SOMO1 and SOMO2 are both singly occupied.

Indeed, Figure 1 shows that the energy differences between the SOMOs are about 5–6 kcal mol^{-1} for the C$_2$Et$_2$- and the C$_2$Me$_2$-bridged systems, while an energy difference of less than 1 kcal mol^{-1} is predicted for the CAAC–diborene system. This explains why singlet ground states are found for the former but a triplet ground state for the latter. Experimental data for the S–T gap of the twisted structure of **CAAC_Full_H_Cl** are not available because its planar structure is much more stable than its twisted structure. However, theory allows inclusion of this system in the investigation. Astonishingly, NEVPT2 predicts that the twisted forms of **CAAC_Mod_H_Cl** and **CAAC_Mod_H_H** have triplet ground states (Table 2). The UMN12L computations predict negligible S–T gaps for both the model systems (Table 2) and the full systems (Table 1). The difference for the systems with alkylated C$_2$R$_2$ bridges can again be reduced to the energy difference of the two SOMOs (Figure 1). For **CAAC_Mod_H_Cl** it is less than 1 kcal mol^{-1}, which explains its triplet ground state.

This large variation arises because on replacing, for example, CH$_3$ with H, SOMO1 is destabilized, while SOMO2 is stabilized. In fact, closer inspection of the phases of the B–CAAC π system shows that they even cross (see Figure 1 and Figures S2–S4 of the Supporting Information). For all alkyl substituents the lower SOMO consists of the bonding linear combination of the π systems of the B–CAAC units, while the upper SOMO contains the antibonding combination. For SOMO1, the inner C$_2$(CH$_3$)$_2$ contribution represents a linear combination of two σ C–CH$_3$ bonds. This linear combination has the correct symmetry to interact with the π systems of the B–CAAC units and is antibonding with respect to both π systems. For SOMO2 the CH σ bonds also contribute, and clearly destabilize this orbital. For the C$_2$H$_2$ bridge this CH–σ destabilizing contribution is missing. Inspection of the phases of the π systems of the B-CAAC units shows that the energy order of the two SOMOs is reversed and the energy difference becomes smaller. Consequently, the triplet becomes the ground state.
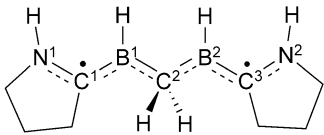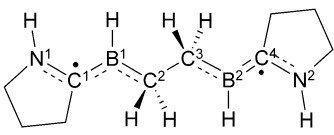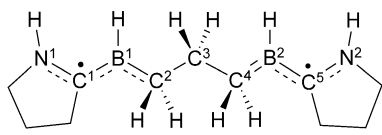
The substituents at both boron centers do not considerably influence the size of the S–T gap (Table 2). On replacing X = Cl with H, the computed S–T gaps remain approximately 0.4–0.5 kcal mol^{-1}. This may result because these substituents do not influence the inner part of the SOMOs (see for example Figure S2 of the Supporting Information), so that the orbital energy differences do not change strongly. Figure 1 compares the SOMOs obtained for the bridged compounds with those of the nonbridged, twisted diborane congeners. In this triplet-ground-state system, the interaction between the CAAC π orbitals is diminished because the B–CAAC moieties are rotated with respect to each other. Nevertheless, the energy difference between the two SOMOs is 1.6 kcal mol^{-1}. This energy gap is larger than those calculated for the C$_2$H$_2$-bridged systems, for example, **CAAC_Mod_H_Cl** or **CAAC_Mod_H_H**.

In another picture, the interaction between the spin centers is responsible for the energy order of singlet and triplet. If the two centers cannot interact, the triplet state is the ground state. If the interaction increases, one singlet state (bonding character between both spin centers) is stabilized while the other is destabilized (antibonding character). If the interaction is sufficiently strong, the stabilized singlet state becomes more stable than the triplet. However, for the given examples this picture is misleading, because the alkylated C$_2$R$_2$ bridge likely hampers the interaction between the two spin centers more than the simple C$_2$H$_2$ bridge.

The orientation and distance between the spin centers are important structural properties that can influence the relative energy of singlet and triplet states, and thus affect the ground-state multiplicity of the molecular system. However, the fact that a preference for triplet states is observed for twisted **CAAC_Mod_H_Cl** and **CAAC_Mod_H_H**, whereas their counterparts featuring methyl-substituted C$_2$R$_2$ bridges have singlet states, indicates that the rules determining singlet or triplet ground states are more complicated, at least for the bridged boron systems studied herein. To shed more light on these complicated relationships, we computed molecules in which two B–CAAC spin centers are connected by the saturated hydrocarbon bridges CH$_2$, (CH$_2$)$_2$, and (CH$_2$)$_3$ in their staggered orientation. The computation of these systems allows insights into the role of distance and orientation, because the saturated hydrocarbon bridge cannot interact with the spin centers, regardless of their orientation. Additionally, they also provide some understanding of the special role of unsaturated bridges described above. The NEVPT2 results are summarized in Table 3.

Table 3. NEVPT2 computations of saturated hydrocarbon-bridged systems to investigate the influence of the relative orientation of radical centers on the multiplicity of the ground state.[a]


bridge	CH$_2$		C$_2$H$_4$		C$_3$H$_6$	
dihedral angle	φ(B^{1}C^{2}B^{2}C^3)		φ(C^{2}C^{3}B^{2}C^4)		φ(C^{3}C^{4}B^{2}C^5)	
dihedral angle	180°	90°	180°	90°	180°	90°
S–T gap	0.71	−0.21	0.22	−0.05	0.05	0.00

[a] The S–T gap [kcal mol^{-1}] is the singlet–triplet gap obtained from NEVPT2(2,2)/cc-pVDZ calculations (for more explanation, see text or Supporting Information). Negative S–T gaps indicate that the system has a triplet ground state.

Chemistry–A European Journal

Full Paper
doi.org/10.1002/chem.202004619

Chemistry Europe
European Chemical
Societies Publishing

According to our calculations, for these systems the relative orientation of the B–CAAC moieties exclusively determines the preferred multiplicity. All systems in which the two B–CAAC moieties are perpendicular to each other have a triplet ground state. This even holds for the CH_2-bridged system, in which the two boron centers are only 2.6 Å apart. In contrast, for all systems with parallel alignments the computations predict a singlet state. Even for the $(CH_2)_3$-bridged system, in which the boron centers are 5.3 Å apart, our computations predict a singlet ground state. These findings underline the special role of the C_2R_2 bridge in the twisted conformers of **CAAC_Mod_H_Cl** and **CAAC_Mod_H_H**. Although the boron centers in these systems are only 4.0–4.1 Å apart, and both spin centers are oriented in a parallel fashion, the computations still predict the triplet state to be lower than the singlet state for this conformer. More information about orbital shapes and energies, as well as the relationship between the form of the MOs (localized versus delocalized) and the wave functions of the saturated hydrocarbon-bridged molecules, are given in the Supporting Information (Sections II and III).

Differences in the properties of NHCs and CAACs, such as the tendency of CAACs to stabilize radicals and biradicals, are usually discussed in terms of their greater π-donating and σ-accepting properties. However, very few studies have closely examined the differences between CAACs and NHCs.[33] We recently contributed to this topic by comparing the properties of CAAC- and NHC-stabilized diborenes[14] and a diboraanthracene.[12] As mentioned above, both showed considerable differences in their geometrical structures and electronic characters. For the diborenes, in addition to steric effects, the differences also result from the triplet states of the CAAC compounds lying considerably lower in energy than those of the corresponding NHC systems. These low-lying triplet states result from smaller HOMO–LUMO gaps, which could be traced back to a more favorable nodal structure for the LUMO of the CAAC compounds. To investigate the generality of these trends, we attempted to synthesize NHC-based diboron compounds with unsaturated C_2 bridges, but without success. To shed some light on this important issue we characterized the corresponding NHC compounds by means of computation. The corresponding geometrical parameters are given in Table S7–S9 of the Supporting Information. The energies are summarized in Table S10 of the Supporting Information.

The main results are summarized in Figure 2, which reveals that the differences found for diborenes are also present in the C_2R_2-bridged compounds. While **CAAC_Full_CH₃_Cl** has an open-shell singlet ground state in which the C_2R_2 bridge is twisted with respect to the B–CAAC moieties, the analogous NHC derivative **NHC_Full_CH₃_Cl** has a closed-shell singlet ground state, and the triplet state lies 8.3 kcal mol⁻¹ higher in energy (Figure 2a). The equilibrium geometry is neither planar nor twisted. In contrast, the C^{NHC}-BCCB-C^{NHC} backbone adopts a helicoidal form (Figure 2b). This geometry seems to balance the steric demands of the various bulky groups with the possibility of forming a π system that is delocalized over the whole backbone (Figure 2c).
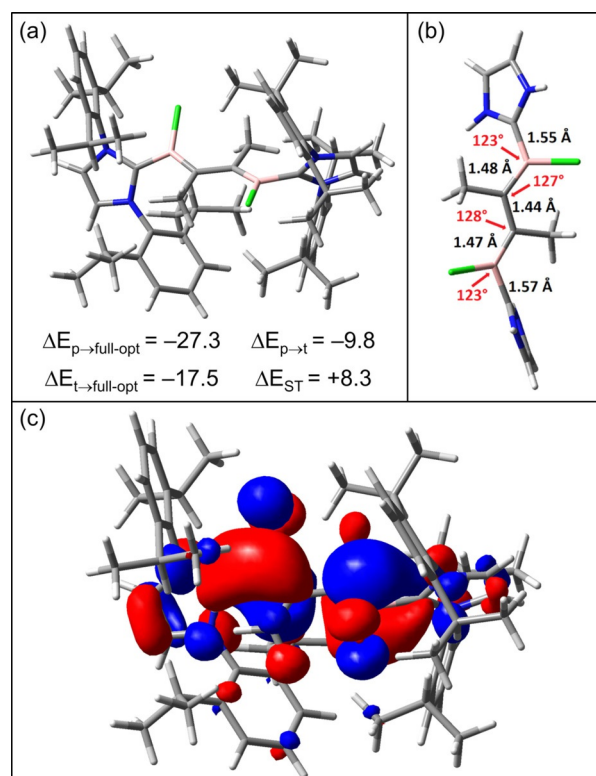
Figure 2. Structure and energies [UMN12L/6–311G(d,p)] of **NHC_Full_CH₃_Cl**. a) Full system and selected relative energies [kcal mol⁻¹]. The S–T gap ΔE_{ST} is the adiabatic one of the fully optimized (full-opt) structures. b) The substituents are omitted for clarity and some geometrical parameters are indicated (bond lengths in Å). c) HOMO of **NHC_Full_CH₃_Cl** (full-opt structure). For more information, see text.

The underlying reason for the different behavior of **NHC_Full_CH₃_Cl** in comparison to **CAAC_Full_CH₃_Cl** is again the higher-lying triplet state of the NHC compounds. This becomes obvious from Table S11 of the Supporting Information, which compares $\Delta E_{p\to t}$ and the S–T gaps of the planar model systems for which the steric effects are diminished. The corresponding orbital energies and shapes are also given. For **CAAC_Mod_CH₃_Cl**, the planar structure is about 4 kcal mol⁻¹ more stable than the twisted one. The triplet state of the planar structure lies approximately 11 kcal mol⁻¹ higher than the singlet.

For **NHC_Mod_CH₃_Cl** the S–T gap of the planar structure is approximately 22 kcal mol⁻¹, that is, about 11 kcal mol⁻¹ higher than that of **CAAC_Mod_CH₃_Cl**. The additional triplet-state destabilization experienced by **NHC_Mod_CH₃_Cl** in comparison to its corresponding CAAC system is also reflected in its higher $\Delta E_{p\to t}$ value, whereby the planar structure is favored by about 7 kcal mol⁻¹ (NHC: $\Delta E_{p\to t} \approx +11$ kcal mol⁻¹) with respect to that of **CAAC_Mod_CH₃_Cl** (CAAC: $\Delta E_{p\to t} \approx +4$ kcal mol⁻¹). As discussed above for diborenes, the increase in the S–T gap again seems to result from stronger destabilization of the LUMO if CAAC and NHC systems are compared. The similarities between the various systems become obvious from the shapes of HOMO−1, HOMO, and LUMO (Table S11 of the Supporting Information).

Chemistry–A European Journal

Full Paper
doi.org/10.1002/chem.202004619

Chemistry
Europe

European Chemical
Societies Publishing

The variations in the steric demands of the C_2 bridge and the boron substituents of the full NHC systems resemble those found for CAAC systems (Tables S10 of the Supporting Information). In both cases, if the alkyl groups at the C_2R_2 bridge are replaced with hydrogen atoms, our computations predict that virtually planar structures are formed. The equilibrium geometry of **NHC_Full_CH$_3$_H** again resembles that of **NHC_Full_CH$_3$_Cl**, while that of **NHC_Full_H_H** is again nearly planar. This shows that—also for the NHC compounds—the methyl groups of the C_2 bridge would be mainly responsible for the distorted equilibrium geometries. More information is provided in the Supporting Information (Section IV).

As previously mentioned, attempts to synthesize the corresponding NHC-based compounds were unsuccessful. To shed some light on the factors precluding their experimental realization, we computed the thermodynamics of the CAAC-to-NHC exchange reaction (Scheme 2). The computed reaction energies for the various systems are summarized in Table S12 (Supporting Information Section V). Our UMN12L/6-311G(d,p) computations indicate that the exchange reaction energy is only about 4 kcal mol^{-1} for X = Cl and R^2 = CH$_3$. The reaction energy is slightly lower ($\approx$ 3 kcal mol^{-1}) for R^2 = H, while that for R^2 = C$_2$H$_5$ is higher (10 kcal mol^{-1}). This indicates that for R$_2$ = CH$_3$ and H, the difficulties in the synthesis of the NHC compounds are mainly due to kinetic effects. In contrast, for R$_2$ = C$_2$H$_5$ thermodynamic effects seem to be more important.
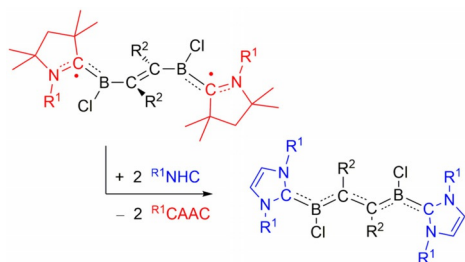
Scheme 2. Conceptual exchange reaction of CAAC substituents with NHC substituents. R^1 = Dip and R^2 = C$_2$H$_5$, CH$_3$, H.

Conclusion

We have applied DFT and high-level multireference calculations to explore the steric and electronic effects at play in the planar and twisted structures of C_2R_2-bridged boron-based biradicals. The recently synthesized CAAC-stabilized diboron compounds with alkyl-substituted unsaturated C_2 bridges showed unexpected geometrical and electronic structures that were not fully understood at the time. Without strain effects, one would expect a planar orientation of the two B–CAAC moieties and the C_2 bridge, because it would allow a π-delocalized system with a closed-shell ground state. However, alkyl-substituted C_2R_2 bridges twist by about 90° with respect to both B–CAAC units, and an open-shell singlet ground state results. While the unusual geometrical and electronic properties of the molecules were unambiguously determined, the underlying reasons remained unclear, especially the interplay between steric effects

induced by the various groups, delocalization effects through the C_2R_2 bridge, and the energy gap between open- and closed-shell structures, which motivated the present work.

Our analysis shows that the steric demands of the CAAC and chloro substituents are necessary to induce the twisting of the structure in systems containing the $C_2(CH_3)_2$ bridge, while those containing the $C_2(C_2H_5)_2$ bridge twist even without the presence of substituents at CAAC. For the C_2H_2 bridge a planar structure with a closed-shell ground state is formed even in the presence of the other bulky groups, that is, the presence of alkyl groups at the C_2 bridge is essential to induce a twisted structure. By replacing the various substituents with hydrogen atoms, we could quantify the distinct effects that contribute. Delocalization through the C_2 bridge provides a stabilization of approximately 27 kcal mol^{-1}. For alkyl-substituted bridges this stabilizing effect is overcompensated by the much stronger influence of the steric effects induced by the substituents at CAAC and by the chlorine atoms, which amount to at least 60–70 kcal mol^{-1}. These effects are so strong that they induce sp^3 hybridization of the carbon centers of the C_2R_2 bridge, imposing a biradical character on the system. On relaxing the geometry, an open-shell singlet structure is favored, in which the C_2R_2 bridge is twisted with respect to the B–CAAC units. This clarifies that for an alkyl-substituted C_2R_2 bridge, steric effects are the dominant player. In contrast, the significant negation of steric demands in systems with non-alkylated C_2H_2 bridges leads to the dominance of delocalization effects, resulting in planar structures.

We also investigated the effects determining the preference for singlet or triplet multiplicities in these systems. According to our computations, the preferred open-shell singlet multiplicity for alkyl-substituted, twisted C_2R_2 bridges results from the energy gap between the two SOMOs. These consist of the bonding and antibonding linear combination of π orbitals of the CAAC moieties but are modulated by participation of the σ framework of the unsaturated C_2 bridge. For the alkyl substituents, this contribution increases the energy difference between the SOMOs by destabilizing the orbital comprising the antibonding combination. In contrast, for the hydrogen-substituted C_2R_2 bridges the antibonding combination is stabilized by a contribution from the CH-σ system, so that the bonding and antibonding orbitals cross and a small energy gap results. This ultimately leads to a triplet ground state for the compound with a twisted C_2H_2 bridge. The replacement of the unsaturated C_2R_2 bridge with saturated CH$_2$, (CH$_2$)$_2$, and (CH$_2$)$_3$ bridges allowed us to underline the unusual role of the former.

Finally, we investigated the thermodynamic consequences of replacing the CAAC ligands with appropriate NHCs. Our computations indicate that kinetic effects are mainly responsible for the elusiveness of the corresponding NHC-stabilized systems with unsaturated C_2R_2 (R = H, CH$_3$) bridges, whereas for R = C$_2$H$_5$, thermodynamic effects also play a significant role. We believe that the findings discussed herein will contribute to the experimental development of novel boron-based biradicals.

Chemistry–A European Journal

Full Paper
doi.org/10.1002/chem.202004619

Chemistry
Europe
European Chemical
Societies Publishing

Acknowledgements

Conflict of interest

The authors declare no conflict of interest.

Keywords: ab initio calculations · boron · carbene ligands · density functional calculations · radicals

[1] a) E. Krause, *Ber. Dtsch. Chem. Ges.* **1924**, *57*, 216–217; b) E. Krause, H. Polack, *Ber. Dtsch. Chem. Ges.* **1926**, *59*, 777–785; c) A. Berndt, H. Klusik, K. Schlüter, *J. Organomet. Chem.* **1981**, *222*, c25–c27; d) H. Klusik, A. Berndt, *Angew. Chem. Int. Ed. Engl.* **1981**, *20*, 870–871; *Angew. Chem.* **1981**, *93*, 903–904; e) H. Klusik, A. Berndt, *J. Organomet. Chem.* **1982**, *232*, C21–C23; f) W. Kaim, A. Schulz, *Angew. Chem. Int. Ed. Engl.* **1984**, *23*, 615–616; *Angew. Chem.* **1984**, *96*, 611–612; g) M. M. Olmstead, P. P. Power, *J. Am. Chem. Soc.* **1986**, *108*, 4235–4236; h) J. J. Eisch, T. Dluzniewski, M. Behrooz, *Heteroat. Chem.* **1993**, *4*, 235–241; i) C. J. Harlan, T. Hascall, E. Fujita, J. R. Norton, *J. Am. Chem. Soc.* **1999**, *121*, 7274–7275; j) J. D. Hoefelmeyer, F. P. Gabbaï, *J. Am. Chem. Soc.* **2000**, *122*, 9054–9055; k) R. J. Kwaan, C. J. Harlan, J. R. Norton, *Organometallics* **2001**, *20*, 3818–3820; l) W. Kaim, N. S. Hosmane, S. Záliš, J. A. Maguire, W. N. Lipscomb, *Angew. Chem. Int. Ed.* **2009**, *48*, 5082–5091; *Angew. Chem.* **2009**, *121*, 5184–5193.

[2] Y. Su, R. Kinjo, *Coord. Chem. Rev.* **2017**, *352*, 346–378.

[3] a) V. Lavallo, Y. Canac, C. Präsang, B. Donnadieu, G. Bertrand, *Angew. Chem. Int. Ed.* **2005**, *44*, 5705–5709; *Angew. Chem.* **2005**, *117*, 5851–5855; b) V. Lavallo, Y. Canac, A. DeHope, B. Donnadieu, G. Bertrand, *Angew. Chem. Int. Ed.* **2005**, *44*, 7236–7239; *Angew. Chem.* **2005**, *117*, 7402–7405.

[4] a) J. D. Masuda, W. W. Schoeller, B. Donnadieu, G. Bertrand, *Angew. Chem. Int. Ed.* **2007**, *46*, 7052–7055; *Angew. Chem.* **2007**, *119*, 7182–7185; b) D. Martin, M. Soleilhavoup, G. Bertrand, *Chem. Sci.* **2011**, *2*, 389–399; c) U. S. D. Paul, U. Radius, *Chem. Eur. J.* **2017**, *23*, 3993–4009; d) M.-A. Légaré, G. Bélanger-Chabot, R. D. Dewhurst, E. Welz, I. Krummenacher, B. Engels, H. Braunschweig, *Science* **2018**, *359*, 896–900; e) M.-A. Légaré, M. Rang, G. Bélanger-Chabot, J. I. Schweizer, I. Krummenacher, R. Bertermann, M. Arrowsmith, M. C. Holthausen, H. Braunschweig, *Science* **2019**, *363*, 1329–1332; f) M.-A. Légaré, C. Pranckevicius, H. Braunschweig, *Chem. Rev.* **2019**, *119*, 8231–8261.

[5] a) D. S. Weinberger, M. Melaimi, C. E. Moore, A. L. Rheingold, G. Frenking, P. Jerabek, G. Bertrand, *Angew. Chem. Int. Ed.* **2013**, *52*, 8964–8967; *Angew. Chem.* **2013**, *125*, 9134–9137; b) C. D. Martin, M. Soleilhavoup, G. Bertrand, *Chem. Sci.* **2013**, *4*, 3020; c) P. Bissinger, H. Braunschweig, A. Damme, I. Krummenacher, A. K. Phukan, K. Radacki, S. Sugawara, *Angew. Chem. Int. Ed.* **2014**, *53*, 7360–7363; *Angew. Chem.* **2014**, *126*, 7488–7491; d) P. Jerabek, H. W. Roesky, G. Bertrand, G. Frenking, *J. Am. Chem. Soc.* **2014**, *136*, 17123–17135; e) J. Böhnke, H. Braunschweig, W. C. Ewing, C. Hörl, T. Kramer, I. Krummenacher, J. Mies, A. Vargas, *Angew. Chem. Int. Ed.* **2014**, *53*, 9082–9085; *Angew. Chem.* **2014**, *126*, 9228–9231; f) K. Chandra Mondal, S. Roy, H. W. Roesky, *Chem. Soc. Rev.* **2016**, *45*, 1080–1111; g) S. Roy, K. C. Mondal, H. W. Roesky, *Acc. Chem. Res.* **2016**, *49*, 357–369; h) M. Arrowsmith, H. Braunschweig, M. A. Celik, T. Dellermann, R. D. Dewhurst, W. C. Ewing, K. Hammond, T. Kramer, I. Krummenacher, J. Mies, K. Radacki, J. K. Schuster, *Nat. Chem.* **2016**, *8*, 890–894; i) S. Kundu, S. Sinhababu, S. Dutta, T. Mondal, D. Koley, B. Dittrich, B. Schwederski, W. Kaim, A. C. Stückl, H. W. Roesky, *Chem.*

Commun. **2017**, *53*, 10516–10519; j) B. Li, S. Kundu, A. C. Stückl, H. Zhu, H. Keil, R. Herbst-Irmer, D. Stalke, B. Schwederski, W. Kaim, D. M. Andrada, G. Frenking, H. W. Roesky, *Angew. Chem. Int. Ed.* **2017**, *56*, 397–400; *Angew. Chem.* **2017**, *129*, 407–411; k) M. Arrowsmith, J. D. Mattock, J. Böhnke, I. Krummenacher, A. Vargas, H. Braunschweig, *Chem. Commun.* **2018**, *54*, 4669–4672; l) M. M. Hansmann, M. Melaimi, D. Munz, G. Bertrand, *J. Am. Chem. Soc.* **2018**, *140*, 2546–2554; m) M. M. Hansmann, M. Melaimi, G. Bertrand, *J. Am. Chem. Soc.* **2018**, *140*, 2206–2213; n) S. Sinhababu, S. Kundu, M. M. Siddiqui, A. N. Paesch, R. Herbst-Irmer, B. Schwederski, P. Saha, L. Zhao, G. Frenking, W. Kaim, D. Stalke, H. W. Roesky, *Chem. Commun.* **2019**, *55*, 4534–4537; o) S. Kundu, S. Sinhababu, V. Chandrasekhar, H. W. Roesky, *Chem. Sci.* **2019**, *10*, 4727–4741; p) S. K. Mellerup, Y. Cui, F. Fantuzzi, P. Schmid, J. T. Goettel, G. Bélanger-Chabot, M. Arrowsmith, I. Krummenacher, Q. Ye, V. Engel, B. Engels, H. Braunschweig, *J. Am. Chem. Soc.* **2019**, *141*, 16954–16960; q) W. Li, S. Kundu, C. Köhler, J. Li, S. Dutta, Z. Yang, D. Stalke, R. Herbst-Irmer, A. C. Stückl, B. Schwederski, D. Koley, W. Kaim, H. W. Roesky, *Organometallics* **2019**, *38*, 1939–1945; r) S. Hagspiel, M. Arrowsmith, F. Fantuzzi, A. Hermann, V. Paprocki, R. Drescher, I. Krummenacher, H. Braunschweig, *Chem. Sci.* **2020**, *11*, 551–555; s) R. Jazzar, M. Soleilhavoup, G. Bertrand, *Chem. Rev.* **2020**, *120*, 4141–4168.

[6] a) V. M. Marx, A. H. Sullivan, M. Melaimi, S. C. Virgil, B. K. Keitz, D. S. Weinberger, G. Bertrand, R. H. Grubbs, *Angew. Chem. Int. Ed.* **2015**, *54*, 1919–1923; *Angew. Chem.* **2015**, *127*, 1939–1943; b) X. Hu, M. Soleilhavoup, M. Melaimi, J. Chu, G. Bertrand, *Angew. Chem. Int. Ed.* **2015**, *54*, 6008–6011; *Angew. Chem.* **2015**, *127*, 6106–6109; c) E. A. Romero, R. Jazzar, G. Bertrand, *J. Organomet. Chem.* **2017**, *829*, 11–13; d) B. L. Tran, J. L. Fulton, J. C. Linehan, J. A. Lercher, R. M. Bullock, *ACS Catal.* **2018**, *8*, 8441–8449; e) B. L. Tran, J. L. Fulton, J. C. Linehan, M. Balasubramanian, J. A. Lercher, R. M. Bullock, *ACS Catal.* **2019**, *9*, 4106–4114.

[7] a) D. Bourissou, O. Guerret, F. P. Gabbaï, G. Bertrand, *Chem. Rev.* **2000**, *100*, 39–92; b) W. A. Herrmann, *Angew. Chem. Int. Ed.* **2002**, *41*, 1290–1309; *Angew. Chem.* **2002**, *114*, 1342–1363; c) H. Zhao, Z. Lin, T. B. Marder, *J. Am. Chem. Soc.* **2006**, *128*, 15637–15643; d) Y. Segawa, M. Yamashita, K. Nozaki, *Angew. Chem. Int. Ed.* **2007**, *46*, 6710–6713; *Angew. Chem.* **2007**, *119*, 6830–6833; e) U. Radius, F. M. Bickelhaupt, *Coord. Chem. Rev.* **2009**, *253*, 678–686; f) M. Melaimi, M. Soleilhavoup, G. Bertrand, *Angew. Chem. Int. Ed.* **2010**, *49*, 8810–8849; *Angew. Chem.* **2010**, *122*, 8992–9032; g) M. A. Celik, R. Sure, S. Klein, R. Kinjo, G. Bertrand, G. Frenking, *Chem. Eur. J.* **2012**, *18*, 5676–5692; h) M. Wagner, T. Zöller, W. Hiller, M. H. Prosenc, K. Jurkschat, *Chem. Eur. J.* **2013**, *19*, 9463–9467; i) B. M. Day, T. Pugh, D. Hendriks, C. F. Guerra, D. J. Evans, F. M. Bickelhaupt, R. A. Layfield, *J. Am. Chem. Soc.* **2013**, *135*, 13338–13341; j) W. Yang, D. Ma, Y. Zhou, X. Dong, Z. Lin, J. Sun, *Angew. Chem. Int. Ed.* **2018**, *57*, 12097–12101; *Angew. Chem.* **2018**, *130*, 12273–12277.

[8] a) H. G. Viehe, Z. Janousek, R. Merenyi, L. Stella, *Acc. Chem. Res.* **1985**, *18*, 148–154.

[9] a) T. Zeng, N. Ananth, R. Hoffmann, *J. Am. Chem. Soc.* **2014**, *136*, 12638–12647; b) T. Stuyver, T. Zeng, Y. Tsuji, S. Fias, P. Geerlings, F. De Proft, *J. Phys. Chem. C* **2018**, *122*, 3194–3200; c) T. Stuyver, T. Zeng, Y. Tsuji, P. Geerlings, F. De Proft, *Nano Lett.* **2018**, *18*, 7298–7304; d) T. Stuyver, D. Danovich, S. Shaik, *J. Phys. Chem. A* **2019**, *123*, 7133–7141; e) S. Kröncke, C. Herrmann, *J. Chem. Theory Comput.* **2019**, *15*, 165–177.

[10] J. Böhnke, T. Dellermann, M. A. Celik, I. Krummenacher, R. D. Dewhurst, S. Demeshko, W. C. Ewing, K. Hammond, M. Heß, E. Bill, E. Welz, M. I. S. Röhr, R. Mitrić, B. Engels, F. Meyer, H. Braunschweig, *Nat. Commun.* **2018**, *9*, 1197.

[11] A. Deissenberger, E. Welz, R. Drescher, I. Krummenacher, R. D. Dewhurst, B. Engels, H. Braunschweig, *Angew. Chem. Int. Ed.* **2019**, *58*, 1842–1846; *Angew. Chem.* **2019**, *131*, 1857–1861.

[12] C. Saalfrank, F. Fantuzzi, T. Kupfer, B. Ritschel, K. Hammond, I. Krummenacher, R. Bertermann, R. Wirthensohn, M. Finze, P. Schmid, V. Engel, B. Engels, H. Braunschweig, *Angew. Chem. Int. Ed.* **2020**, *59*, 19338–19343.

[13] J. W. Taylor, A. McSkimming, C. F. Guzman, W. H. Harman, *J. Am. Chem. Soc.* **2017**, *139*, 11032–11035.

[14] E. Welz, J. Böhnke, R. D. Dewhurst, H. Braunschweig, B. Engels, *J. Am. Chem. Soc.* **2018**, *140*, 12580–12591.

[15] J. Poater, M. Solà, F. M. Bickelhaupt, *Chem. Eur. J.* **2006**, *12*, 2889–2895.

[16] R. Peverati, D. G. Truhlar, *Phys. Chem. Chem. Phys.* **2012**, *14*, 13171.

[17] a) R. Krishnan, J. S. Binkley, R. Seeger, J. A. Pople, *J. Chem. Phys.* **1980**, *72*, 650–654; b) A. D. McLean, G. S. Chandler, *J. Chem. Phys.* **1980**, *72*,

5639–5648; c) M. M. Francl, W. J. Pietro, W. J. Hehre, J. S. Binkley, M. S. Gordon, D. J. DeFrees, J. A. Pople, *J. Chem. Phys.* **1982**, *77*, 3654–3665.

[18] a) C. Brückner, B. Engels, *J. Phys. Chem. A* **2015**, *119*, 12876–12891; b) C. Brückner, F. Würthner, K. Meerholz, B. Engels, *J. Phys. Chem. C* **2017**, *121*, 4–25.

[19] a) B. Engels, S. D. Peyerimhoff, *J. Phys. Chem.* **1989**, *93*, 4462–4470; b) V. Pless, H. U. Suter, B. Engels, *J. Chem. Phys.* **1994**, *101*, 4042–4048.

[20] a) V. Settels, W. Liu, J. Pflaum, R. F. Fink, B. Engels, *J. Comput. Chem.* **2012**, *33*, 1544–1553; b) C. Brückner, B. Engels, *Chem. Phys.* **2017**, *482*, 319–338.

[21] a) B. Engels, *Theor. Chim. Acta* **1993**, *86*, 429–437; b) H. U. Suter, M.-B. Huang, B. Engels, *J. Chem. Phys.* **1994**, *101*, 7686–7691.

[22] a) C. Angeli, R. Cimiraglia, S. Evangelisti, T. Leininger, J.-P. Malrieu, *J. Chem. Phys.* **2001**, *114*, 10252–10264; b) C. Angeli, R. Cimiraglia, J.-P. Malrieu, *Chem. Phys. Lett.* **2001**, *350*, 297–305; c) C. Angeli, R. Cimiraglia, J.-P. Malrieu, *J. Chem. Phys.* **2002**, *117*, 9138–9153.

[23] a) T. H. Dunning, *J. Chem. Phys.* **1989**, *90*, 1007–1023; b) D. E. Woon, T. H. Dunning, *J. Chem. Phys.* **1993**, *98*, 1358–1371.

[24] B. O. Roos, *Adv. Chem. Phys. Ab Initio Methods Quantum Chem. Part 2, Vol. 69* (Ed.: K. P. Lawley), Wiley, **1987**, pp. 399–445.

[25] J. R. Schmidt, N. Shenvi, J. C. Tully, *J. Chem. Phys.* **2008**, *129*, 114110.

[26] a) K. Yamaguchi, *Chem. Phys. Lett.* **1975**, *33*, 330–335; b) S. Yamanaka, M. Okumura, M. Nakano, K. Yamaguchi, *J. Mol. Struct.* **1994**, *310*, 205–218; c) M. Nakano, *Top. Curr. Chem.* **2017**, *375*, 47.

[27] Gaussian 16, Revision A.03, M. J. Frisch, G. W. Trucks, H. B. Schlegel, G. E. Scuseria, M. A. Robb, J. R. Cheeseman, G. Scalmani, V. Barone, B. Mennucci, G. A. Petersson, H. Nakatsuji, M. Caricato, X. Li, H. P. Hratchian, A. F. Izmaylov, J. Bloino, G. Zheng, J. L. Sonnenberg, M. Hada, M. Ehara, K. Toyota, R. Fukuda, J. Hasegawa, M. Ishida, T. Nakajima, Y. Honda, O. Kitao, H. Nakai, T. Vreven, J. A. Montgomery, Jr., J. E. Peralta, F. Ogliaro, M. Bearpark, J. J. Heyd, E. Brothers, K. N. Kudin, V. N. Staroverov, R. Kobayashi, J. Normand, K. Raghavachari, A. Rendell, J. C. Burant, S. S. Iyengar, J. Tomasi, M. Cossi, N. Rega, J. M. Millam, M. Klene, J. E. Knox, J. B. Cross, V. Bakken, C. Adamo, J. Jaramillo, R. Gomperts, R. E. Stratmann, O. Yazyev, A. J. Austin, R. Cammi, C. Pomelli, J. W. Ochterski, R. L. Martin, K. Morokuma, V. G. Zakrzewski, G. A. Voth, P. Salvador, J. J. Dannenberg, S. Dapprich, A. D. Daniels, Ö. Farkas, J. B. Foresman, J. V. Ortiz, J. Cioslowski, D. J. Fox, Gaussian Inc., Wallingford CT, **2016**.

[28] F. Neese, *Wiley Interdiscip. Rev.: Comput. Mol. Sci.* **2012**, *2*, 73–78.

[29] J. Autschbach, M. Srebro, *Acc. Chem. Res.* **2014**, *47*, 2592–2602.

[30] a) V. Moha, W. Leitner, M. Hölscher, *Chem. Eur. J.* **2016**, *22*, 2624–2628; b) N. Mardirossian, M. Head-Gordon, *J. Chem. Theory Comput.* **2016**, *12*, 4303–4325.

[31] A. Deissenberger, *Dibortetrahalogenide Für Die Darstellung Neuer Borhaltiger Verbindungen in Niedrigen Oxidationsstufen*, Julius-Maximilians-Universität Würzburg, **2019**.

[32] a) V. Bonačić-Koutecký, J. Koutecký, J. Michl, *Angew. Chem. Int. Ed. Engl.* **1987**, *26*, 170–189; *Angew. Chem.* **1987**, *99*, 216–236; b) J. Michl, V. Bonačić-Koutecký, *Tetrahedron* **1988**, *44*, 7559–7585.

[33] a) K. C. Mondal, H. W. Roesky, M. C. Schwarzer, G. Frenking, I. Tkach, H. Wolf, D. Kratzert, R. Herbst-Irmer, B. Niepötter, D. Stalke, *Angew. Chem. Int. Ed.* **2013**, *52*, 1801–1805; *Angew. Chem.* **2013**, *125*, 1845–1850; b) N. Holzmann, D. M. Andrada, G. Frenking, *J. Organomet. Chem.* **2015**, *792*, 139–148.